Characterization of an indoor environmental chamber and identification of C_1-C_4 OVOCs during isoprene ozonolysis

Yan Tan[1], Chang Liu[2], Kinfai Ho[3], Qingxin Ma[4], Shun-cheng Lee[1,*]

[1] *Department of Civil and Environmental Engineering, The Hong Kong Polytechnic University, Hong Kong, China*

[2] *State Key Laboratory of Severe Weather & Key Laboratory of Atmospheric Chemistry of China Meteorological Administration, Chinese Academy of Meteorological Sciences, Beijing 100081, China;*

[3] *School of Public Health and Primary Care, The Chinese University of Hong Kong, Shatin, Hong Kong, China*

[4] *Research Center for Eco-Environmental Sciences, Chinese Academy of Sciences, Beijing 100085, China*

Correspondence authors:

Prof. Shun-cheng Lee, E-mail: ceslee@polyu.edu.hk, Telephone: +852 2766 6011, Fax: +852 2334 6389

Abstract

An environmental chamber was built up and characterized at The Hong Kong Polytechnic University. The chamber consists of a 6 m^3 poly tetrafluoroethylene-co-perfluoropropyl vinyl ether (PFA) Teflon film reactor inside a stainless-steel enclosure stocked with a series of online gas-phase and aerosol-phase analytical instruments. Temperature and relative humidity (RH) are controllable and can be set to a range of 10 ~ 40 ± 1°C and 5 ~ 85%, ± 3%, respectively. An air purification system provides zero air for chamber with total volatile organic compounds (VOCs) < 1 ppb, NO_X and O_3 < 1 ppb and particles concentration < 10^2 particles·cm^{-3}. Characterization experiments were performed under dry conditions (RH < 5%) and ambient temperature (25°C). The average wall loss rates of O_3 and NO_2 were observed to be 2.92 × 10^{-6} s^{-1} and 9.3 × 10^{-4} s^{-1} respectively, and particle wall loss rate was 0.27 h^{-1}. Dark ozonolysis of isoprene was studied using this chamber and the production of C_1~C_4 oxygenated volatile organic compounds (OVOCs) such as formaldehyde, methacrolein (MACR) and methyl vinyl ketone (MVK) were identified using Proton-Transfer-Reaction Time-of-Flight Mass Spectrometry (PTR-TOF-MS). The results of experiments indicate that this new facility can be used to investigate and simulate the gaseous chemistry and secondary aerosol formation.

Key Words: Environmental chamber, Chamber characterization, Isoprene, Ozone, OVOCs

Introduction

As a useful tool to investigate and infer the chemical mechanism and kinetics, environmental chamber is widely used in past few decades. In order to study the pollutants in atmospheric chemistry, smog chamber was immersed in work from the 1980s.[1-3] Volatile organic compounds (VOCs) can react with different active radicals such as hydroxyl radicals (OH), nitrate radicals (NO_3), and ozone (O_3) in atmosphere. Those complex chemical reactions will form some intermediates that represent one or more polar functional groups such as aldehyde, ketone, alcohol, nitro, peroxyl nitrate, hydroperoxide and so on. These intermediates tend to be less volatile and could easily transfer to the particulate phase to form secondary organic aerosol (SOA). Meanwhile, some second-generation products can also be further oxidized. An effective test and scientific prediction are necessary to understand the pathway and mechanism of VOCs/free radicals reactions. However, as there are thousands of VOCs species in the ambient, not only the large number of intertwined reactions, but also the meteorological conditions can have an unpredictable impact on these reactions. So, we cannot obtain scientific and reasonable pathway and mechanism through observing real atmosphere. Atmospheric chemical processes are affected by meteorological conditions, which makes difficult to conduct targeted research. However, temperature, humidity, light, precursor concentration and even the meteorological factors can be controlled in chamber simulation experiment. Therefore, a chamber simulation experiment is an effective way to study the

mechanism of atmospheric pollution and further develop solutions for pollution control.

Seinfeld and his colleagues[4, 5] set up a 65 m^3 fluorinated ethylene propylene (FEP) - materialled outdoor smog chamber at California Institute of Technology (Caltech) for aerosol formation from photooxidation of biogenic and aromatic hydrocarbons in 1980s. So far, many chamber systems have been developed to study the gas-phase products as well as the secondary organic aerosol formation. University of California, Riverside (UCR) has been working on chamber for nearly 40 years and eight different outdoor and indoor chambers have been constructed.[6-8] Through years of experimentation and characterization, UCR established a more functional chamber system which consists of two collapsible 90 m^3 FEP Teflon film reactors.[9, 10] Another representative smog chamber EUPHORE was a double hemispherical reactor located in Valencia, Spain, focusing on atmospheric chemical reactions in the gas phase and also the kinetic parameters.[11, 12]

In China, smog chamber facilities have been developed since 1980s.[13-17] These studies have provided valuable experience for the development of smog chamber to study kinetics and mechanisms for photochemistry. Recently, in order to meet the challenges of air pollution control in China, some new chamber systems have been developed.[13, 18, 19]

Biogenic volatile organic compounds (BVOC) emit into atmosphere from plants source, which is the key factor to affect the atmospheric environment. The reaction of BVOC and active radical leads to the generation of secondary organic aerosol (SOA) and

particulate matter (PM) sequentially.[20] Isoprene (2-methyl-1,3-butadiene, C_5H_8) is the most abundant hydrocarbon except methane in global atmospheric emissions with an estimated emission at ~400-660 Tg yr^{-1}.[21-23] Due to its two double bonds and highly emitted concentration, C_5H_8 can react with free radicals e.g. OH radicals, NO_3 radicals and O_3 easily and hence plays an important role in atmospheric chemistry.[24-26]

This work describes the first indoor environmental chamber which was newly established at The Hong Kong Polytechnic University (PolyU). This chamber facility is designed to study formation mechanisms of the reactions of isoprene and free radicals as well as the contribution to SOA, and to serve as a platform for evaluating the performance of newly developed online gas or particle monitors, such as Proton-Transfer-Reaction Time-of-Flight Mass Spectrometry. A set of characterization experiments were performed correspondingly to evaluate the performance of the new facility. Meanwhile, investigating of gas-phase products of isoprene oxidation in dark was also conducted in this chamber under different conditions.

Materials and methods

Facility description

The indoor walk-in environmental chamber comprises a 18.26 m^3 stainless steel enclosure and a 6 m^3 Teflon bag as reactor inside at PolyU. In order to achieve the condition such as temperature and humidity controllable during the simulation, the chamber system has been constructed with box-in-box design. All the reactions complete within the 0.127 mm-thick Teflon PFA bag. Figure 1 shows the brief schematic diagram of the PolyU environmental chamber.

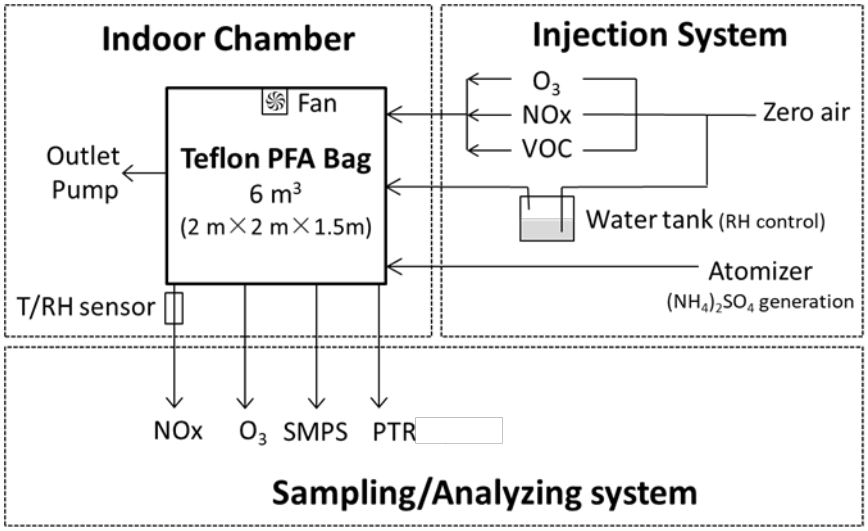

Figure 1. Schematic of the PolyU environmental chamber.

Enclosure

The Teflon reactor is housed in an environmental chamber make by stainless-steel (3.2 m × 3.2 m × 2.5 m) and the effective volume of this stainless-steel is 18.26 m^3.[27] The material of the inner walls is insulated stainless steel sheet. The facility has its own air conditioner and can help adjust Teflon reactor's temperature (T) by a central control system, which can be set to a range of 10 ~ 40 ± 1°C. Water purification system including clean water tank, water level safety switch and water heating element provides clean water for relative humidity (RH) control, which is located behind the stainless-steel enclosure and can be set to a range of 5 ~ 85%, ± 3% RH. And a sensor (HBO; Incorporated, USA) is equipped inside the Teflon reaction to ensure that the temperature and RH are within the required range.

Teflon reactor

The reactor of chamber system can be made of different materials, such as Al alloy,[28] stainless steel,[29, 30] or FEP Teflon film.[9, 13, 31] Because of the chemical characteristic and

low interfacial free energy, Teflon does not participate in chemical reactions easily, and has a very small adsorption capacity for particulate matter. So, most of the smog chambers used for chemical simulation are consist of Teflon film. Similarly like other fluoropolymers such as Teflon PTFE poly (tetrafluoroethylene) and FEP (fluorinated ethylene-propylene co-polymer), PFA (poly(tetrafluoroethylene-co-perfluoropropyl vinyl ether)) have been extensively used as material for chamber[32-34] for its aggressive chemicals, as well as corrosion-resistant lining of vessels. The volume of our Teflon bag is 6 m^3 i.e. 2 m (Length) × 2 m (Width) × 1.5 m (Height) and was fabricated from 0.127 mm-thick Teflon PFA film. A stainless-steel frame was settled to mount the whole reactor bag with four parallel belt loops. A homogeneous mixing of reactants can be achieved by installing a mixing fan at the centre of the chamber ceiling.

There are five Teflon ports and one access port on the reactor. Four of the Teflon ports are used for reagents injection such as zero air, VOC sample (such as isoprene), ozone and seed aerosol. Another hole is used for sampling and connected with an array of instruments. The access port is housed on the back side of reactor bag. The access port is 0.5 m away from the chamber floor and designed for emergency circumstances. All these ports are equipped with Kynar tube fittings and re-inforced with Teflon to keep seal.

Air purification system

An air cleaning system provided the zero air by introducing clean dry air. This purification system equipped with activated charcoal particle filters and High-Efficiency Particulate Air (HEPA) filters to remove gaseous organics and particles

146 respectively. The flow rate of zero air was set to 12 dm^3/min. The standard of
147 background air was kept < 1 ppb for individual VOC, < 1 ppb NO_X, O_3 and no
148 detectable particles. The chamber was flushed continuously for over 48 hours with
149 clean air before use.

150 *Injection system*

151 Gaseous reactants (like O_3 and NO_2) were injected via a non-absorbent tube, which was
152 connected with one of the Teflon port on the left side of reactor. Ozone, generated by a
153 commercial ozone generator (Jelight Model 2001; Jelight Company, USA) with
154 ultraviolet light was connected to the adjacent Teflon port. The gas injection volume
155 can be calculated by the injection duration time and air flow rate. For liquid reactants,
156 a heating system was used to generate and inject gasified reactants within an air bag
157 which contained known volume liquid sample. Seed particles generated by an atomizer
158 (TSI 3079; TSI Incorporated, USA) passed through a silicone tube to remove water and
159 eliminate the charge before introducing into the reactor.

160 *Instrumentation*

161 A variety of gas-phase and aerosol-phase instruments employed to investigate the
162 different species are briefly described and listed in Table 1. All instruments were located
163 close to the chamber and connected to the sampling port of inner reactor.

164 Ozone was investigated by a photometric ozone analyser (Teledyne 400E; Teledyne
165 API, USA), which sampled at the flow rate of 0.8 dm^3/min ± 10%. Model 200E
166 nitrogen oxide analyser (Teledyne 200E; Teledyne API, USA) was used to measure
167 the concentration of NO, NO_2 and NOx, and the sampling flow rate was 0.5 dm^3/min

± 10%. The instruments were calibrated weekly and the detection limits are also listed in Table 1.

As an advanced technology, Proton-Transfer-Reaction Time-of-Flight Mass Spectrometry (PTR-TOF-MS) has also been used in many chamber studies.[35-37] The atmospheric process can be simulated in a large chamber by controlling air conditions (temperature, relative humidity, light, air exchange rate etc.) and known levels of certain air pollutants like NOx, ozone, and aerosols. Here we applied PTR-TOF-MS (IONICON, Austria) to detect the concentration of VOCs in real time. The PTR-TOF-MS 1000 ultra combines the latest evolution with the new funnel technology to improve ion transmission leading to a much higher sensitivity, which is as low as 5 ppt. This online VOCs monitoring instrument can be easily used in high-speed applications, even under the situation of very low VOC concentrations, complex samples or a large number of sample compounds as well. The PTR-TOF-MS was calibrated weekly by zero air and standard gas (Gas canister, Restek, USA)

For aerosol monitoring, particle number concentrations and size distributions are obtained from scanning mobility particle sizer (SMPS) (TSI 3080; TSI Incorporated, USA). Aerosol sampling flow rate was 3.0 dm^3/min, and the size distribution range from 15 ~ 680 nm was measured within 240 s. The accuracy of the particle number concentration is ± 10%.

Table 1. List of equipment for chamber.

Instrument	Species	Flow rate	Lower Detectable Limit	Max range
Teledyne 400E	O_3	0.8 dm^3/min ± 10%	0.6 ppb	10,000 ppb
Teledyne 200E	$NO/NO_2/NO_x$	0.5 dm^3/min ± 10%	0.5 ppb	20,000 ppb
PTR-TOF-MS 1000	VOCs	0.8 dm^3/min	5 ppt	10,000 amu
TSI 3080	particle number concentrations/ size distributions	0.3 dm^3/min ± 10%	10 nm	10^8 particles (cm^3) at 10 nm

Results and discussion

Characterization of the new chamber system is necessary and significant to identify the performance of chamber and to understand future experiment results. So the impact of reactor walls on gas-phase reactivity and secondary aerosol formation is discussed.

Wall loss of gases

During the experimental process in environmental chamber, loss of gaseous reactants and products might happen on the inner surface of the reactor, due to deposition effect or conversion to other species.[38] The correction factor of wall loss is important in explaining experimental results and parameterizing simulation results and it is required to calculate the accurate SOA yield. The wall loss process is generally considered to be a first order kinetic process, and the equation of its reaction rate is expressed by Equation (1),[39]

$$\frac{d[\mathrm{X}]}{dt} = -K_{w,x}[\mathrm{X}] \quad (1)$$

where [X] is the concentration of the target compound, and $-K_{w,x}$ is wall loss rate constant of the target compound.

In order to determine the constant of wall loss rate for O_3, NO_2 and representative BVOC isoprene, different experiments were carried out. The objective species, i.e. O_3, NO_2 and isoprene, were injected into the chamber respectively. Each concentration was monitored continuously in the dark condition. Figure 2 shows the change of concentration and its index curve with time. All the index curves have a good correlation with time, where R^2 is 0.979, 0.932 and 0.991 respectively, indicating that wall loss is a first order kinetics process.

Owing to the significant role played in atmospheric chemistry, the wall loss of gaseous in the smog chamber has been widely studied. Table 2 summaries the wall loss rate constants of gases of the PolyU environmental chamber in comparison with other smog chambers. Table 2 shows that the wall loss rates of our chamber are all reasonable and at a relative low level compared with the value of other reported smog chambers. Wall loss factor of isoprene in our work is 2.8×10^{-7} (lifetime is 52.08 d), which was the smallest compared with other species and can be omitted.

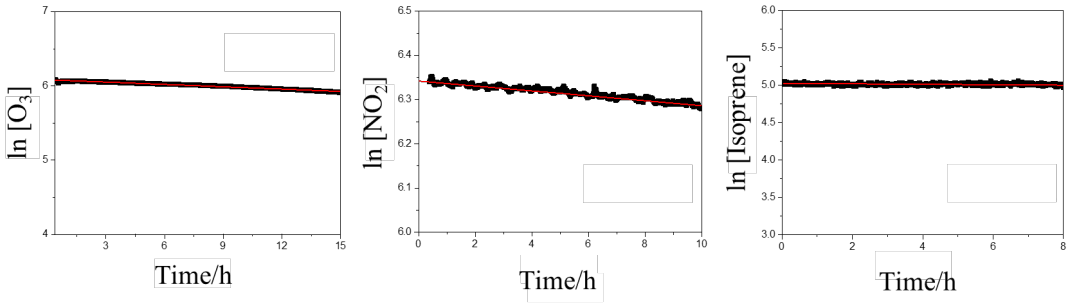

Figure 2. Index curve of concentration and reaction time for (a) O_3, (b) NO_2 and (c)

isoprene.

Table 2. Comparison of wall loss rate of gas species between PolyU chamber and other chamber systems.

Institution	Volume (m^3)	Material	k (s^{-1})		References
			O_3	NO_2	
GIG-CAS	35	Teflon FEP	2.2×10^{-6}	1.4×10^{-4}	Wang, Liu, Bernard, Ding, Wen, Zhang, Zhang, He, Lü and Chen [13]
ERT	3.9	Teflon FEP	3×10^{-6}	$0\sim5\times10^{-4}$	Rollins, Kiendler-Scharr, Fry, Brauers, Brown, Dorn, Dube, Fuchs, Mensah and Mentel [40]
Tsinghua	2	Teflon FEP	1×10^{-6}	4.2×10^{-4}	Wu, Lü, Hao, Zhao, Li, Takekawa, Minoura and Yasuda [17]
PolyU	6	Teflon PFA	2.92×10^{-6}	9.3×10^{-4}	This work

Particle wall loss

Wall loss of the suspended particles in the environmental chamber are caused by several reasons, including electrostatic action, turbulence, Brownian diffusion and gravitational

sedimentation. The accurate evaluation of particulate matters lost on the surface of the reactor is necessary to obtain the total mass of the product. Particle wall loss rate is proportional to the initial concentration of particulate matters, and it is also affected by particle size. The wall loss rate of the particles can be described by the first order kinetic Equation (2),[39]

$$\frac{dN(d_p,t)}{dt} = -k(d_p) \times N(d_p,t) \quad (2)$$

where $N(d_p,t)$ is the concentration of the particles, d_p is the diameter of the particles, $k(d_p)$ is wall loss rate constant of particles.

In order to evaluate the wall loss rate constant of the smog chamber, aerosol generator (0.5 mol/L $(NH_4)_2SO_4$ solution) with a certain concentration atomization flow of $(NH_4)_2SO_4$ was introduced into the smog chamber. Meanwhile, the distribution of the particle size is measured by SMPS continuously. The distribution of particle size of $(NH_4)_2SO_4$ was the reactor is shown in Figure 3.

According to the relationship between the total concentration of particulate matter and time, the constant of wall loss rate of the total particle concentration can be obtained. As shown in Figure 3, $(NH_4)_2SO_4$ seed was injected into chamber at the beginning of experiment. After the injection, particles appeared with an average diameter of 100 nm. Owing to coagulation behaviour of smaller particles and probably higher wall loss rate of smaller particles, the smaller particles decreased and turned into 250 nm in the following hours.

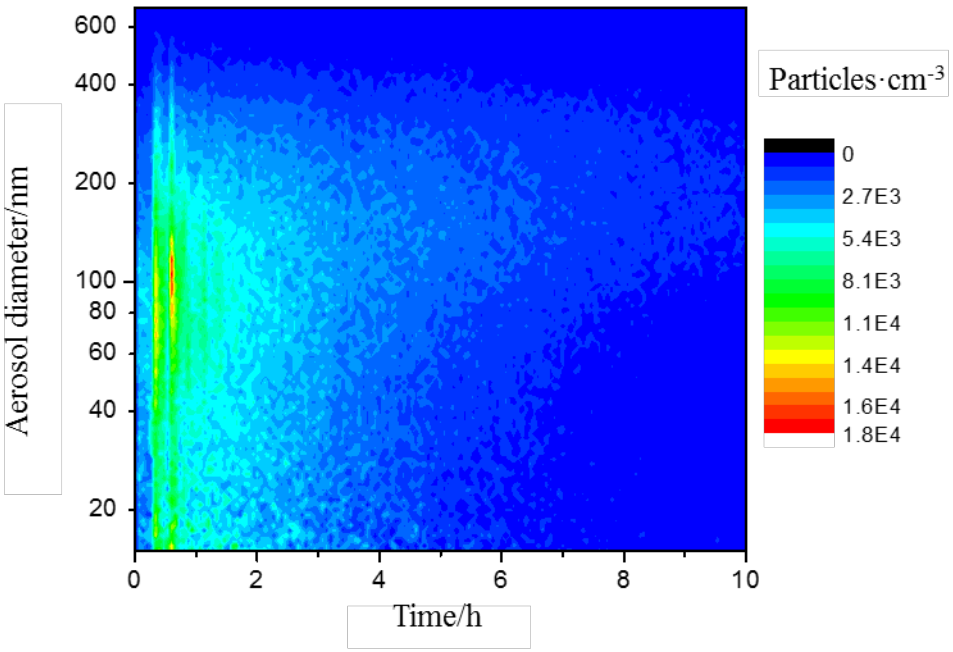

Figure 3. The distribution of particle size of $(NH_4)_2SO_4$ in chamber.

The relationship between the constant of wall loss rate of particle concentration and particle size is fitted by using below the Equation (3),[41]

$$\text{kdep}(dp) = a \times d_p^b + \frac{c}{d_p^d} \quad (3)$$

which is for cuboid chamber, and the value of a, b, c and d for this work can be suggested as in a = 6.52×10^{-2}, b = 7.55×10^{-2}, c = 41.21 and d = 1.19, respectively. The particle wall loss rate constant for PolyU chamber is 0.2674 h^{-1} from this equation. Figure 4 compares the particle wall loss rate between PolyU chamber and other reported chamber experiments. The constant of wall loss rate in our work is close to other experiments,[13, 17, 41] and is lower than the result of Takekawa's work.[41] Lower wall loss rates of not only gas species but also particles show stable existence of gases and small wall loss of particles.

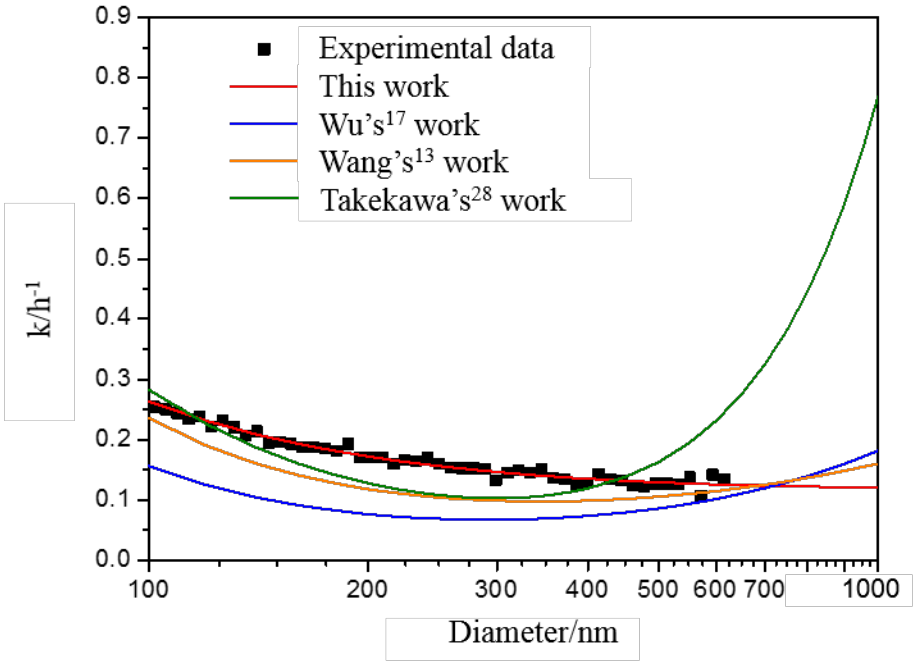

Figure 4. Comparison of particle wall loss rate between PolyU chamber and other chamber systems.

Identification of OVOCs

Using this well-designed chamber system, isoprene dark ozonolysis experiments was carried out. In this experiment, 66 ppb of isoprene was first injected into the chamber, followed by the introduction of 440 ppb O_3 under dry conditions (RH < 5%) with temperature at 25 ± 1°C. Figure 5(a) and (b) show the mass spectrometry of gaseous products obtained by PTR-TOF-MS. At the beginning of the experiment, m/z 69, as the signal of isoprene, was identified in Figure 5(a) with red bar. The peak of isoprene was disappeared after 6-hours reaction with an excess of ozone, accompanied by other peaks (see the black bars in Figure 5(a)). It indicated that the reaction of isoprene with ozone produces a series of gaseous products. In Figure 5(a), strong ion signals of m/z 31, 47, 59, 61 and 71 were detected at the end of isoprene dark ozonolysis. To further

identify and confirm these peaks, the specific mass spectra of gaseous products with formula were listed in Figure 5(b). The strongest peak at m/z 31 was identified as formaldehyde. Besides, the higher ion signal of 71 was attributed to Methacrolein (MACR) and methyl vinyl ketone (MVK). There are two pathways for isoprene ozonolysis to form ozonides by adding ozone to the carbon-carbon double bond. And every ozonide can decomposes to the mentioned products. As discussed in many other studies, MVK and MACR is the major first-generation product.[42, 43] Hence, all these are the major oxidation products from the reaction of isoprene initiated by ozone [44]. Additionally, a battery of energetic Criegee intermediates were formed during the reaction following the ion signals at m/z 47, 61, 75 and 87, which are attributed to CH_2O_2, $C_2H_4O_2$, $C_3H_6O_2$ and $C_4H_6O_2$, respectively. These OVOCs are all C_1~C_4 species and could be classified into aldehyde, ketone, and acid (or ester), as summarized in Table 3. And the results are basically agreed with previous chamber studies and model simulations.[40, 45, 46]

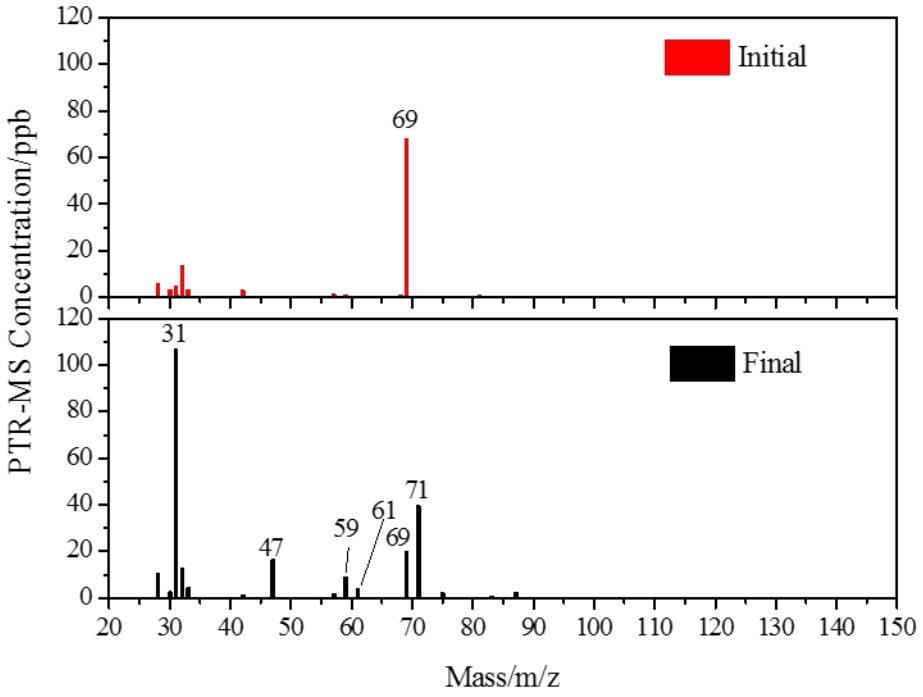
Initial
Final
PTR-MS Concentration/ppb
Mass/m/z
69
31
47
59
61
69
71

287

288 (a)

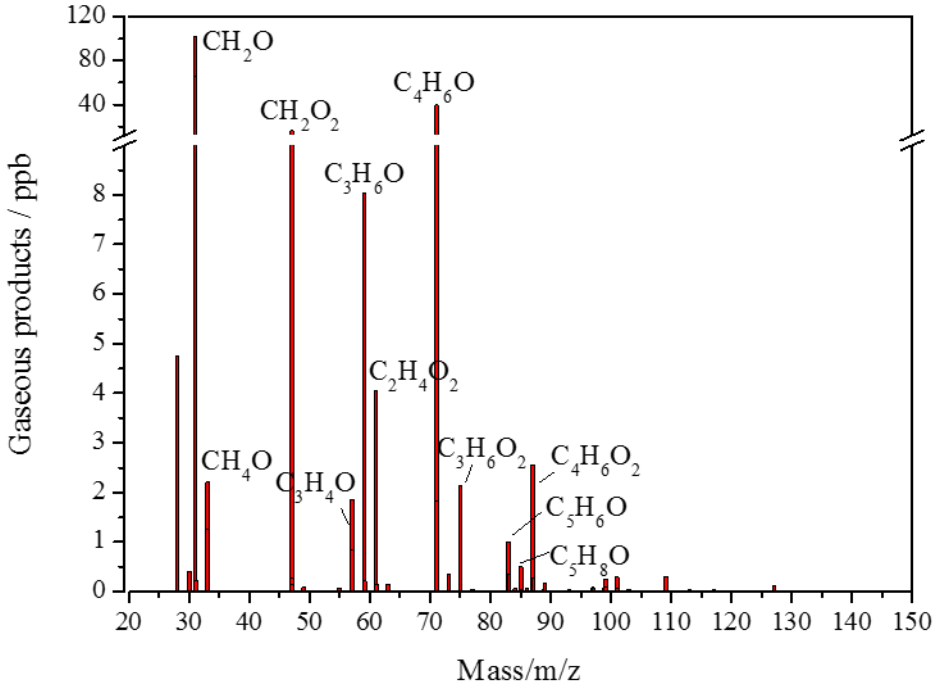
Gaseous products / ppb
Mass/m/z
CH2O
CH2O2
C4H6O
C3H6O
C2H4O2
CH4O
C3H4O
C3H6O2
C4H6O2
C5H6O
C5H8O

289

(b)

Figure 5. Mass spectra of gaseous products detected by PTR-TOF-MS. (a) Different in mass spectra before and after the reaction. (b) Mass spectra of gaseous products of isoprene reaction with O_3.

Table 3. Summary of C_1~C_4 OVOCs detected during the dark ozonolysis of isoprene

Category	Aldehyde $(CH_3)_nCHO$		Ketone $(CH_3)_nCO$		Acid/Ester $C_nH_{2n}O_2$			
Formula	CH_2O	C_4H_6O	C_3H_6O	C_4H_6O	CH_2O_2	$C_2H_4O_2$	$C_3H_6O_2$	$C_4H_6O_2$
Structure	HCHO	MACR: $CH_3C=CH_2CHO$	CH_3COCH_3	MVK: $CH_3COCH=CH_2$	HCOOH	CH_3COOH	CH_3CH_2COOH	$CH_3COOCH=CH_2$

Effect of relative humidity on OVOCs formation

Due to the diversification of meteorological and geographical conditions, the relative humidity (RH) in the real atmosphere is also different. To investigate how increases in RH affect C_1~C_4 OVOCs formation and yield, a series of experiments were carried out (details given in Table 4.) RH was varied over a range of < 5% to 56% in the isoprene-ozone system, and the initial mixing ratios of isoprene and O_3 were approximate to 1. Yields of gaseous species were calculated as C atom by following Equation (4),[47]

$$Y = \frac{\Delta[\mathrm{HC}]}{\Delta[isoprene]} \quad (4)$$

where Δ[HC] is calculated according to the consumption of total VOCs (TVOCs), Δ[isoprene] is the reduced amount of isoprene. Figure 6 shows the yields of major gaseous species under different RH conditions during the reaction of isoprene with

ozone. The curves of CH_2O_2, $C_2H_4O_2$, C_3H_6O, $C_3H_6O_2$, C_4H_6O and $C_4H_6O_2$ are nearly stable. Figure 6 illustrates that except the formaldehyde (HCHO), humidity has little influence on the generation of C_1~C_4 OVOCs. This result has been proved and is readily found in the literature that RH has little effect on the gas-phase production and aerosol yields.[48]For the decrease of formaldehyde, the hydrophilicity property of HCHO might result in the adsorption and transformation of formaldehyde to particle phase.[49]

Table 4. Summary of initial conditions for isoprene ozonolysis under different RH experiments.

Experiment number	Temperature (K)	RH (%)	$[isoprene]_{ini}$ (ppb)	$[O_3]_{ini}$ (ppb)	$[isoprene]_{ini}/[O_3]_{ini}$
1	295 ± 1.1	< 5	98	100	0.98
2	296 ± 0.8	20	89	92	0.97
3	294 ± 1.2	45	70	75	0.93
4	295 ± 0.7	56	98	101	0.97

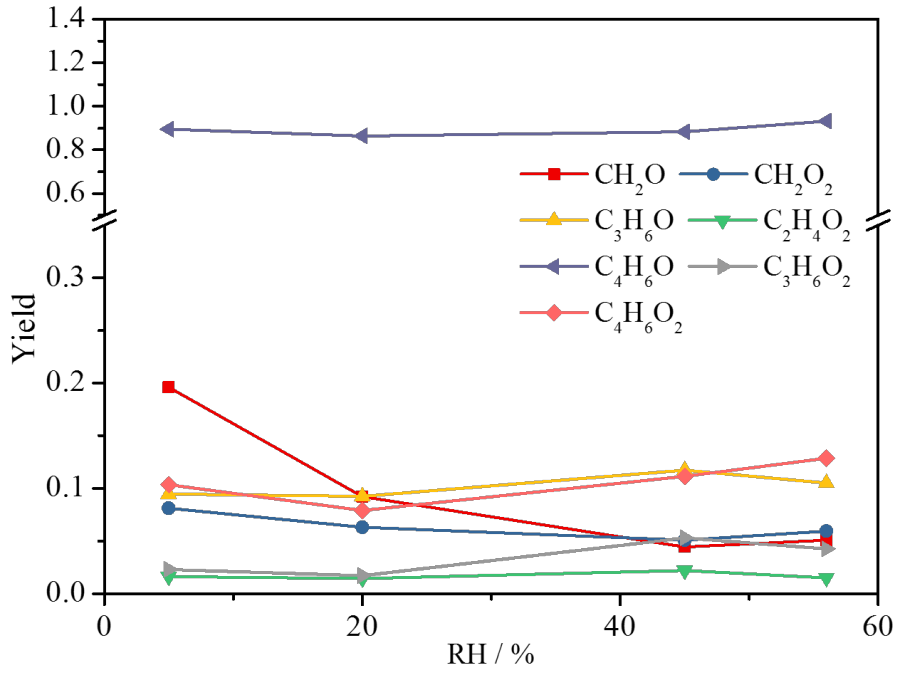

Figure 6. Effect of RH on the OVOCs yields during isoprene dark ozonolysis

However, some researchers believe that RH might affect heterogeneous reactions and gas or particle partitioning.[46, 50, 51] To have a better understanding of RH effect on OVOCs formation, Figure 7 shows a comparison between dry condition (RH < 5%) and humid condition (RH = 56%) in this work for gaseous species. Concentration growth was observed for the products formed in isoprene-ozone reaction system. The concentration of CH_2O_2 decreased from 13.76 ppb to 5.53 ppb with increasing humidity from < 5% to 56%. Ketone products like C_3H_6O and C_4H_6O also have a lower concentration under RH = 56%. Results from different RH experiments suggest that OVOCs formation from isoprene dark ozonolysis should be RH dependent. More generation oxidation products may still contribute to SOA formation due to the effect of liquid water content on SOA yields.

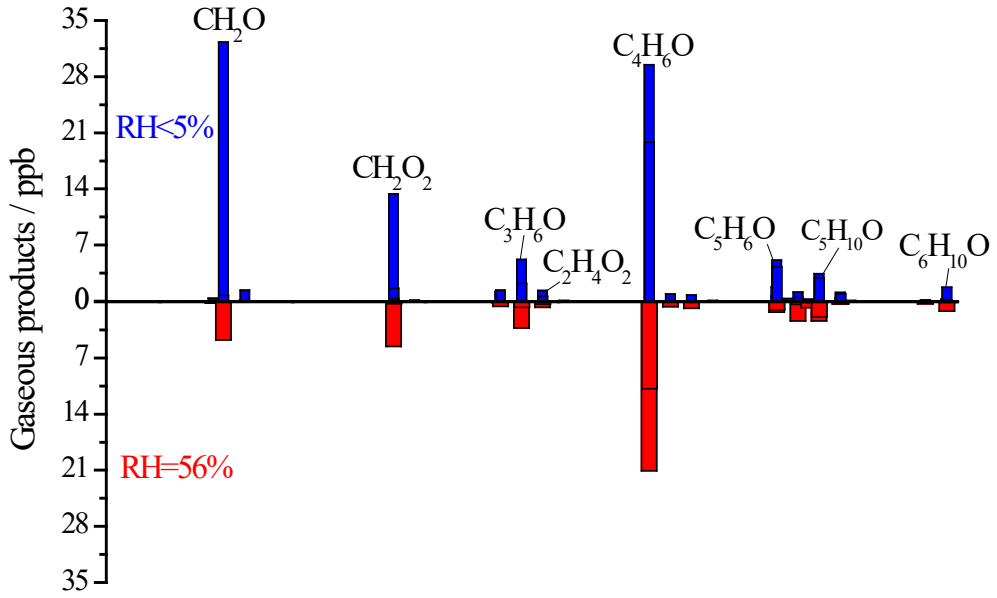

Figure 7. A comparison for gaseous species concentrations between different RH value. Blue bar (upper): RH < 5% and red bar (lower): RH = 56%.

Conclusion

An environmental chamber has been built up at PolyU, and characterization experiments described in this paper demonstrate that our PolyU environmental chamber facility can be used to provide valuable data for gas-phase chemistry and secondary aerosol formation. Observed relatively lower wall loss rates of gas species and particles reflect the long lifetime of these species and small wall effects. Results of isoprene ozonolysis experiments in dark illustrate the chamber's utility for evaluating gas-phase chemical mechanisms. Formation of C_1~C_4 OVOCs was detected using PTR-TOF-MS. The effect of humidity on OVOCs formation were studied. Results showed that in addition to the formaldehyde HCHO, humidity had no

influence on the yields of C_1~C_4 OVOCs, but the concentrations of all these OVOCs decreased under humid condition and may contribute to SOA production.

Authors' contribution

All authors contributed equally in the preparation of this manuscript.

Declaration of conflicting interests

The author(s) declared no potential conflicts of interest with respect to the research, authorship and/or publication of this article.

Funding

This work was supported by The Research Grants Council of Hong Kong Government (Project No. T24/504/17), The Research Grants Council of Hong Kong Government (PolyU152083/14E and PolyU152090/15E), Hong Kong RGC Collaborative Research Fund (C5022-14G).

References

1. Akimoto H, Sakamaki F, Hoshino M, Inoue G and Okuda M. Photochemical ozone formation in propylene-nitrogen oxide-dry air system. *Environ Sci Technol* 1979; 13: 53-58.
2. Carter WPL, Atkinson R, Winer AM and Pitts Jr JN. Experimental investigation of chamber-dependent radical sources. *Int J Chem Kinet* 1982; 14: 1071-1103.
3. Jeffries HE, Kamens RM, Sexton KG and Gerhardt AA. *Outdoor smog chamber experiments to test photochemical models*. 1982 Apr 1 1982. North Carolina Univ., Chapel Hill (USA): School of Public Health.
4. Leone JA and Seinfeld JH. Comparative analysis of chemical reaction mechanisms for photochemical smog. *Atmos Environ* 1985; 19: 437-464.
5. Stern JE, Flagan RC, Grosjean D and Seinfeld JH. Aerosol formation and growth in atmospheric aromatic hydrocarbon photooxidation. *Environ Sci Technol* 1987; 21: 1224-1231.
6. Carter WPL, Pierce JA, Luo D and Malkina IL. Environmental chamber study of maximum incremental reactivities of volatile organic compounds. *Atmos Environ* 1995; 29: 2499-2511.
7. Atkinson R, Carter WP, Darnall KR, Winer AM and Pitts Jr JN. A smog chamber and modeling study of the gas phase NO_x–air photooxidation of toluene and the cresols. *Int J Chem Kinet* 1980; 12: 779-836.
8. Carter WPL, Luo DM and Malkina IL. *Environmental chamber studies for development of an updated photochemical mechanism for VOC reactivity assessment*. California Environmental Protection Agency, Air Resources Board, Research Division: Citeseer, 1997.
9. Carter WPL, Cocker III DR, Fitz DR, Malkina IL, Bumiller K, Sauer CG, Pisano JT, Bufalino C and Song C. A new environmental chamber for evaluation of gas-phase chemical mechanisms and secondary aerosol formation. *Atmos Environ* 2005; 39: 7768-7788.
10. Carter WPL, Fitz D, Cocker III DR, Malkina IL, Bumiller K, Sauer CG, Pisano JT, Bufalino C and Song C. *Development of a Next-Generation Environmental Chamber Facility for Chemical Mechanism and VOC Reactivity Research*. 2005. United States Environmental Protection Agency, California.
11. Martín-Reviejo M and Wirtz K. Is benzene a precursor for secondary organic aerosol? *Environ Sci Technol* 2005; 39: 1045-1054.
12. Becker KH. *The European Photoreactor EUPHORE: Design and Technical Development of the European Photoreactor and First Experimental Results: Final Report of the EC-Project*. 1996.
13. Wang XM, Liu TY, Bernard F, Ding X, Wen S, Zhang YL, Zhang Z, He Q, Lü S and Chen JM. Design and characterization of a smog chamber for studying gas-phase chemical mechanisms and aerosol formation. *Atmos Meas Tech* 2014; 7: 301-313.
14. Wang WX, Xi Y, Lin ZY and Wang H. Study on reaction rate constants of CH_4 and its life-time. *China Environ Sci* 1995; 4.
15. Ren KF, Li JJ, Wang WL and Zhang H. Investigation on experiment system for modeling of photochemical smog. *Acta ScientiaeCircumatantiae* 2005; 25: 1431-1435.
16. Xu YF, Jia L, Ge MF, Du L, Wang GC and Wang DX. A kinetic study of the reaction of ozone with ethylene in a smog chamber under atmospheric conditions. *Chinese Sci Bull* 2006; 51: 2839-2843.
17. Wu S, Lü ZF, Hao JM, Zhao Z, Li JH, Takekawa H, Minoura H and Yasuda A. Construction and characterization of an atmospheric simulation smog chamber. *Adv Atmos Sci* 2007; 24: 250-258.

18. Zhang HF, Ye XN, Cheng TT, Chen JM, Yang X, Wang L and Zhang RY. A laboratory study of agricultural crop residue combustion in China: Emission factors and emission inventory. *Atmos Environ* 2008; 42: 8432-8441.
19. Li K, Wang WG, Ge MF, Li JJ and Wang D. Optical properties of secondary organic aerosols generated by photooxidation of aromatic hydrocarbons. *Sci Rep-UK* 2014; 4: 4922.
20. Li KW, Chen LH, Han K, Lv B, Bao KJ, Wu XC, Gao X and Cen KF. Smog chamber study on aging of combustion soot in isoprene/SO_2/NO_x system: Changes of mass, size, effective density, morphology and mixing state. *Atmos Res* 2017; 184: 139-148.
21. Guenther A, Hewitt CN, Erickson D, Fall R, Geron C, Graedel T, Harley P, Klinger L, Lerdau M and McKay W. A global model of natural volatile organic compound emissions. *J Geophys Res-Atmos* 1995; 100: 8873-8892.
22. Guenther A, Karl T, Harley P, Wiedinmyer C, Palmer P and Geron C. Estimates of global terrestrial isoprene emissions using MEGAN (Model of Emissions of Gases and Aerosols from Nature). *Atmos Chem Phys* 2006; 6: 3181-3210.
23. Liu YJ, Brito J, Dorris MR, Rivera-Rios JC, Seco R, Bates KH, Artaxo P, Duvoisin S, Keutsch FN and Kim S. Isoprene photochemistry over the Amazon rainforest. *Proc Natl Acad Sci* 2016; 113: 6125-6130.
24. Clark CH, Kacarab M, Nakao S, Asa-Awuku A, Sato K and Cocker III DR. Temperature effects on secondary organic aerosol (SOA) from the dark ozonolysis and photo-oxidation of isoprene. *Environ Sci Technol* 2016; 50: 5564-5571.
25. Santos F, Longo K, Guenther A, Kim S, Gu D, Oram D, Forster G, Lee J, Hopkins J and Brito J. Biomass burning emission disturbances of isoprene oxidation in a tropical forest. *Atmos Chem Phys* 2018; 18: 12715-12734.
26. Liu YJ, Kuwata M, McKinney KA and Martin ST. Uptake and release of gaseous species accompanying the reactions of isoprene photo-oxidation products with sulfate particles. *Phys Chem Chem Phys* 2016; 18: 1595-1600.
27. Lee SC and Wang B. Characteristics of emissions of air pollutants from mosquito coils and candles burning in a large environmental chamber. *Atmos Environ* 2006; 40: 2128-2138.
28. Tanaka T, Wada K, Hisamoto J, Sawada H and Matsuura H. *Chamber material made of Al alloy and heater block*. 2003.
29. Wang J, Doussin JF, Perrier S, Perraudin E, Katrib Y, Pangui E and Picquet-Varrault B. Design of a new multi-phase experimental simulation chamber for atmospheric photosmog, aerosol and cloud chemistry research. *Atmos Meas Tech* 2011; 4: 2465.
30. Lee SC, Lam S and Ho KF. Characterization of VOCs, ozone, and PM_{10} emissions from office equipment in an environmental chamber. *Build Environ* 2001; 36: 837-842.
31. Lai CY, Liu YC, Ma JZ, Ma QX and He H. Degradation kinetics of levoglucosan initiated by hydroxyl radical under different environmental conditions. *Atmos Environ* 2014; 91: 32-39.
32. Valente RJ, Thornton FC and Williams EJ. Field comparison of static and flow-through chamber techniques for measurement of soil NO emission. *J Geophys Res-Atmos* 1995; 100: 21147-21152.
33. Rohrer F, Bohn B, Brauers T, Brüning D, Johnen F-J, Wahner A and Kleffmann J. Characterisation of the photolytic HONO-source in the atmosphere simulation chamber SAPHIR. *Atmos Chem Phys* 2005; 5: 2189-2201.
34. Bu XD, Wang TB and Hall G. Determination of halogens in organic compounds by high

resolution inductively coupled plasma mass spectrometry (HR-ICP-MS). *J Anal Atom Spectrom* 2003; 18: 1443-1451.
35. Liu TY, Wang XM, Deng W, Zhang YL, Chu BW, Ding X, Hu QH, He H and Hao JM. Role of ammonia in forming secondary aerosols from gasoline vehicle exhaust. *Scil China Chem* 2015; 58: 1377-1384.
36. Chu BW, Liu YC, Li JH, Takekawa H, Liggio J, Li S-M, Jiang JK, Hao JM and He H. Decreasing effect and mechanism of $FeSO_4$ seed particles on secondary organic aerosol in α-pinene photooxidation. *Environ Pollut* 2014; 193: 88-93.
37. Wang WG, Li K, Zhou L, Ge MF, Hou SQ, Tong SR, Mu YJ and Jia L. Evaluation and application of dual-reactor chamber for studying atmospheric oxidation processes and mechanisms. *Acta Phys-Chim Sin* 2015; 31: 1251-1259.
38. McMurry PH and Grosjean D. Gas and aerosol wall losses in Teflon film smog chambers. *Environ Sci Technol* 1985; 19: 1176-1182.
39. Cocker DR, Flagan RC and Seinfeld JH. State-of-the-art chamber facility for studying atmospheric aerosol chemistry. *Environ Sci Technol* 2001; 35: 2594-2601.
40. Rollins AW, Kiendler-Scharr A, Fry J, Brauers T, Brown SS, Dorn H-P, Dube WP, Fuchs H, Mensah A and Mentel T. Isoprene oxidation by nitrate radical: alkyl nitrate and secondary organic aerosol yields. *Atmos Chem Phys* 2009; 9: 6685-6703.
41. Takekawa H, Minoura H and Yamazaki S. Temperature dependence of secondary organic aerosol formation by photo-oxidation of hydrocarbons. *Atmos Environ* 2003; 37: 3413-3424.
42. Holloway A-L, Treacy J, Sidebottom H, Mellouki A, Daële V, Le Bras G and Barnes I. Rate coefficients for the reactions of OH radicals with the keto/enol tautomers of 2, 4-pentanedione and 3-methyl-2, 4-pentanedione, allyl alcohol and methyl vinyl ketone using the enols and methyl nitrite as photolytic sources of OH. *J Photoch Photobio A* 2005; 176: 183-190.
43. Edney EO, Kleindienst TE and Corse EW. Room temperature rate constants for the reaction of OH with selected chlorinated and oxygenated hydrocarbons. *Int J Chem Kinet* 1986; 18: 1355-1371.
44. Zhang HF, Rattanavaraha W, Zhou Y, Bapat J, Rosen EP, Sexton KG and Kamens RM. A new gas-phase condensed mechanism of isoprene-NO_x photooxidation. *Atmos Environ* 2011; 45: 4507-4521.
45. Kamens RM, Gery MW, Jeffries HE, Jackson M and Cole EI. Ozone–isoprene reactions: Product formation and aerosol potential. *Int J Chem Kinet* 1982; 14: 955-975.
46. Wennberg PO, Bates KH, Crounse JD, Dodson LG, McVay RC, Mertens LA, Nguyen TB, Praske E, Schwantes RH and Smarte MD. Gas-phase reactions of isoprene and its major oxidation products. *Chem Rev* 2018; 118: 3337-3390.
47. Pandis SN, Harley RA, Cass GR and Seinfeld JH. Secondary organic aerosol formation and transport. *Atmospheric Environment Part A General Topics* 1992; 26: 2269-2282.
48. Dommen J, Metzger A, Duplissy J, Kalberer M, Alfarra MR, Gascho A, Weingartner E, Prévôt ASH, Verheggen B and Baltensperger U. Laboratory observation of oligomers in the aerosol from isoprene/NO_x photooxidation. *Geophys Res Lett* 2006; 33.
49. Vlasenko A, Macdonald AM, Sjostedt SJ and Abbatt JPD. Formaldehyde measurements by Proton transfer reaction–Mass Spectrometry (PTR-MS): correction for humidity effects. *Atmos Meas Tech* 2010; 3: 1055-1062.
50. Pankow JF and Chang EI. Variation in the sensitivity of predicted levels of atmospheric organic

particulate matter (OPM). *Environ Sci Technol* 2008; 42: 7321-7329.
51. Volkamer R, Ziemann PJ and Molina MJ. Secondary organic aerosol formation from acetylene (C_2H_2): seed effect on SOA yields due to organic photochemistry in the aerosol aqueous phase. *Atmos Chem Phys* 2009; 9: 1907-1928.